Convergent, Self-Encoded Bead Sensor Arrays in the Design of an Artificial Nose

ARTICLE *in* ANALYTICAL CHEMISTRY · JULY 1999

Impact Factor: 5.64 · DOI: 10.1021/ac981457i · Source: PubMed

4 AUTHORS, INCLUDING:

John S Kauer
Tufts University
100 PUBLICATIONS **5,359** CITATIONS

SEE PROFILE

Anal. Chem. **1999,** *71,* 2192−2198

Convergent, Self-Encoded Bead Sensor Arrays in the Design of an Artificial Nose

Todd A. Dickinson,[†,§] Karri L. Michael,[†] John S. Kauer,[‡] and David R. Walt*[,†]

Department of Chemistry, Tufts University, Medford, Massachusetts 02155, and Department of Neuroscience, Tufts University School of Medicine, Boston, Massachusetts 02111

We report a new approach to designing an artificial nose based on high-density optical arrays that directly incorporate a number of structural and operational features of the olfactory system. The arrays are comprised of thousands of microsphere (bead) sensors, each belonging to a discrete class, randomly dispersed across the face of an etched optical imaging fiber. Beads are recognized and classified after array assembly by their unique, "self-encoded" response pattern to a selected vapor pulse. The high degree of redundancy built into the array parallels that found in nature and affords new opportunities for chemical-sensor signal amplification. Since each bead is independently addressable through its own light channel, it is possible to combine responses from same-type beads randomly distributed throughout the array in a manner reminiscent of the sensory-neuron convergence observed in the mammalian olfactory system. Signal-to-noise improvements of approximately $n^{1/2}$ have been achieved using this method.

"Biomimetics" describes the implementation of biological principles in the design of artificial devices or systems. For many decades, scientists have recognized the power of naturally occurring systems and their utility in guiding the development of certain technologies. One contemporary example of the biomimetic approach is the development of electronic or artificial noses.[1−3] In this rapidly growing field, arrays of semiselective chemical sensors are coupled to pattern recognition schemes (often computational neural networks), paralleling the biological olfactory system in which semiselective olfactory receptors are combined with higher order neural processing. Drawing on a wide range of fields, from chemistry and biology to materials science and chemometrics, the goal of creating an artificial nose represents an integrative approach to device design. The resilience, selectivity, and sensitivity of the olfactory system make it a particularly useful model for chemical-sensor design. Such a versatile sensor could ultimately have applications as widespread as pollution monitoring, medical diagnosis, food quality control, and land-mine detection.

The primary difference between the artificial-nose approaches that have been used to date is the sensor-transduction mechanism. Common types of sensors currently employed are SAW[4] (surface acoustic wave), conducting polymer,[5] metal oxide,[6] MOSFET[7] (metal oxide sensor field-effect transistor), and QCM[8,9] (quartz-crystal microbalance) sensor arrays. Electrochemical-sensor arrays[10] and an approach employing carbon black particles dispersed within different organic polymers have also been used.[11] While these methods represent the inventive application of various chemical and physical phenomena to odor sensing, there are limitations in each. First, sensor reproducibility has been a major concern, both in generating like elements in a single array as well as generating the same elements across arrays; this difficulty can necessitate time-consuming network retraining for each different array. Second, a number of sensor types have relatively slow response times, ranging from a few seconds to up to one minute or more,[12] with cycle times (response and full recovery) that can last as long as several minutes.[13] The sensitivity of sensor arrays also varies widely depending on the approach. Although some reports of sub ppm measurements have appeared in the literature,[14,15] the majority of electronic-nose sensor arrays exhibit detection limits in the low to middle ppm range, precluding their use in a number of low-concentration applications. In addition, the relatively large size of current arrays (typically from 1 to 15 cm^2 for arrays containing between 6 and 30 elements) increases the sampling volume required and hinders miniaturization. Finally, the standard approach to fabricating electronic-nose arrays, regardless of the type of sensors employed, still involves preparation of individual sensing elements and their subsequent

* Corresponding author: (tel.) (617) 627-3470; (fax) (617) 627-3443; (e-mail) dwalt@emerald.tufts.edu.

† Department of Chemistry, Tufts University.

‡ Department of Neuroscience, Tufts University School of Medicine.

§ Currently at Illumina, Inc., San Diego, CA 92122.

(1) Persaud, K.; Dodd, G. *Nature* (*London*) **1982**, *299*, 352.
(2) Shurmer, H. V.; Gardner, J. W. *Sens. Actuators, B* **1992**, *8*, 1.
(3) Dickinson, T. A.; White, J.; Kauer, J. S.; Walt, D. R. *Trends Biotechnol.* **1998**, *16*, 250.
(4) Grate, J. W.; Rose-Pehrsson, S. L.; Venezky, D. L.; Klusty, M.; Wohltjen, H. *Anal. Chem*. **1993**, *65*, 1868.
(5) Gardner, J. W.; Bartlett, P. N. *Sens. Actuators, A* **1995**, *51*, 57.
(6) Hong, H.-K. et al. *Sens. Actuators, B* **1996**, *35−36*, 338.
(7) Lundstrom, I.; Svensson, C.; Spetz, A.; Sundgren, H.; Winquist, F. *Sens. Actuators, B* **1993**, *13−14*, 16.
(8) Carey, W. P.; Beebe, K. R.; Kowalski, B. R. *Anal. Chem*. **1987**, *57*, 1529.
(9) Hierlemann, A.; Weimar, U.; Kraus, G.; Schweizer-Berberich, M.; Gopel, W. *Sens. Actuators, B* **1995**, *26−27*, 126.
(10) Stetter, J. R.; Jurs, P. C.; Rose, S. L. *Anal. Chem*. **1986**, *58*, 860.
(11) Lonergan, M. C. et al. *Chem. Mater*. **1996**, *8*, 2298.
(12) Yokoyama, K.; Ebisawa, F. *Anal. Chem*. **1993**, *65*, 673.
(13) Xing, W.-L.; He, X.-W. *Analyst* (*Cambridge, U.K.*) **1997**, *122*, 587.
(14) Schurmer, H. V.; Corcoran, P.; James, M. K. *Sens. Actuators, B* **1993**, *15−16*, 256.
(15) Gardner, J. W.; Pearce, T. C.; Friel, S.; Bartlett, P. N.; Blair, N. *Sens. Actuators, B* **1994**, *18−19*, 240.

10.1021/ac981457i CCC: $18.00
Published on Web 05/04/1999

placement into a defined array. In this paper we present a new architecture for an artificial nose that has several advantages over existing approaches.

Previously, we have described a vapor-sensing system that employed temporal data from an array of polymer/dye-coated optical fibers.[16] This system represented the union of earlier research involving vapor-detecting optical sensors,[17] optical-sensor arrays,[18] and temporal analysis[19] and modeling[20] work on the olfactory system. Sensors were prepared individually by dip-coating or photopolymerizing different polymers onto the tips of 300-μm diameter single-core fibers. In the present work, these relatively large fiber sensors have been replaced with ~3-μm spherical beads. Solvatochromic dyes (fluorescent dyes that are sensitive to the polarity of their local environment) are introduced into each of the different bead types either through direct adsorption onto the substrate surface (in the case of porous silica beads) or by using solvents that induce bead swelling (in the case of organic polymer-based beads).

The conventional approach to assembling sensors into an array format involves the careful placement of discrete sensing elements onto defined regions of a substrate. This generally requires individual fabrication and spatial deposition of sensing elements and appropriate registration of their position within the array. Several groups have begun to explore different ways to prepare arrays of cross-reactive sensing elements, including the implementation of continuous-sensing surfaces[21,22] and other integrated array formats.[23] The present sensor array employs a new approach to array fabrication recently developed by our laboratory[24] that allows one to prepare an array of different sensing elements in a single step by introducing a mixture of beads into preformed microwells at the distal end of an optical fiber and identifying the beads and their specific locations afterward. To do this, it is necessary to encode each bead (or, in this case, *type* of bead) with a unique signature which can be used later to identify its location. A wide range of encoding schemes are currently employed for similar purposes, particularly in the field of combinatorial chemistry where large libraries of molecules have been synthesized on solid-phase supports. These encoding schemes include molecular[25] and electronic[26] tagging as well as multiwavelength fluorescent-dye encoding.[24]

EXPERIMENTAL SECTION

Materials. Imaging fiber was purchased from the Galileo Electro-Optics Corporation (Sturbridge, MA). Hydrofluoric acid, Nile Red, and ammonium fluoride were purchased from Aldrich (Milwaukee, WI). Porous silica microspheres (Type A) were removed from a LUNA 3-μm HPLC column (Phenomenex, Torrance, CA). Poly(methylstyrene) microspheres were purchased from Bangs Laboratories (Fishers, IN). All solvents used in this study were HPLC grade or better and were used as received from Aldrich.

Microwell fabrication. The imaging fiber was polished using 30-, 12-, 9-, 3-, 1-, and 0.3-μm lapping films. The polished fiber was cleaned by sonicating for 1 min, rinsed, and allowed to dry. The fiber's distal end was submerged in a buffered hydrofluoric acid solution (0.2 g of ammonium fluoride, 100 μL of hydrofluoric acid (50%), and 600 μL of deionized water) for 70s. The fiber was then transferred to a beaker of deionized water to stop the reaction, and swirled for 30s. Finally, the fiber was rinsed under running tap water and sonicated for 2 min to remove any salts formed during etching.

Bead-Sensor Preparation. The silica/Nile Red sensor beads were prepared by passing excess Nile Red/toluene (1 mg/mL) solution over a sample (~20 mg) of the silica beads using suction filtration; the dye adsorbed directly to the silica surface. All nonadsorbed dye was removed by several washings with toluene. Microspheres used for sensor-bead-types B and C (same polymer) were purchased from Bang's Laboratories and dyed by soaking two separate samples of beads in 1 mg/mL toluene solutions of Nile Red and SensiDye (obtained from J. La Clair, Scripps Research Institute, La Jolla, CA), respectively. Toluene swells the beads, allowing dye to diffuse into and become entrapped within the polymer matrix after solvent removal. Beads were washed with methanol several times and then placed into Nanopure water (0.01% Tween 20) for storage. Note: the beads used in this paper were selected in large part because of their commercial availability; however, these beads are usually intended for solution-phase applications such as those mentioned in the text and are not necessarily optimal for vapor sensing. We are currently pursuing the synthesis of different polymer beads that will be particularly well-suited for this purpose.

SEBA Fabrication. Twenty-microliter samples from 0.5 mg/mL stock solutions of each bead type were mixed thoroughly in an Eppendorf tube and vortexed for 2 min. A droplet (0.2 μL) of the mixture was placed onto the distal tip of a vertically clamped, etched imaging fiber and allowed to dry for 5 min. During this time, beads settled randomly into wells, one bead per well. The packing density (number of wells containing a bead) is directly proportional to the bead concentration of the mixture as well as to the number of drops applied. Excess beads were wiped away with a soft, dust-free Q-tip.

Data Collection and Processing. The majority of vapor pulses were generated using a vacuum-controlled sparging apparatus, and data were collected using a custom-built imaging system; both have been described previously.[27] For the low toluene concentration used in Figures 4C−E, a vapor pulse was generated using a Tedlar bag-based gas-dilution system and verified by GC/MS measurements. Sensor temporal responses are normalized in Figures 2 and 3 to demonstrate the similarity in response shape within a bead type (nonnormalized responses show ~10% variability in amplitude for poly(methylstyrene) sensors and ~40% for silica beads). Signal-to-noise ratios of the fluorescence temporal

(16) Dickinson, T. A.; White, J.; Kauer, J. S.; Walt, D. R. *Nature* (*London*) **1996**, *382*, 697.
(17) Barnard, S.; Walt, D. R. *Environ. Sci. Technol.* **1991**, *25*, 1301.
(18) Barnard, S. M.; Walt, D. R. *Nature* (*London*) **1991**, *353*, 338.
(19) Kauer, J. *J. Physiol.* (*London*) **1974**, *243*, 695.
(20) White, J.; Hamilton, K. A.; Neff, S. R.; Kauer, J. S. *J. Neurosci.* **1992**, *12*, 1772.
(21) Lundstrom, I. et al. *Nature* (*London*) **1991**, *352*, 47.
(22) Dickinson, T. A.; White, J.; Kauer J. S.; Walt, D. R. *Anal. Chem.* **1997**, *69*, 3413.
(23) Neaves, P. I.; Hatfield, J. V. *Sens. Actuators, B* **1995**, *26−27*, 223.
(24) Michael, K. L.; Taylor, L. C.; Schultz, S. L.; Walt, D. R. *Anal. Chem.* **1998**, *70*, 1242.
(25) Still, W. C. *Acc. Chem. Res.* **1996**, *29*, 155.
(26) Czarnik, A. W. *Curr. Opin. Chem. Biol.* **1997**, *1*, 60.
(27) White, J.; Kauer, J. S.; Dickinson, T. A.; Walt, D. R. *Anal. Chem.* **1996**, *68*, 2191.

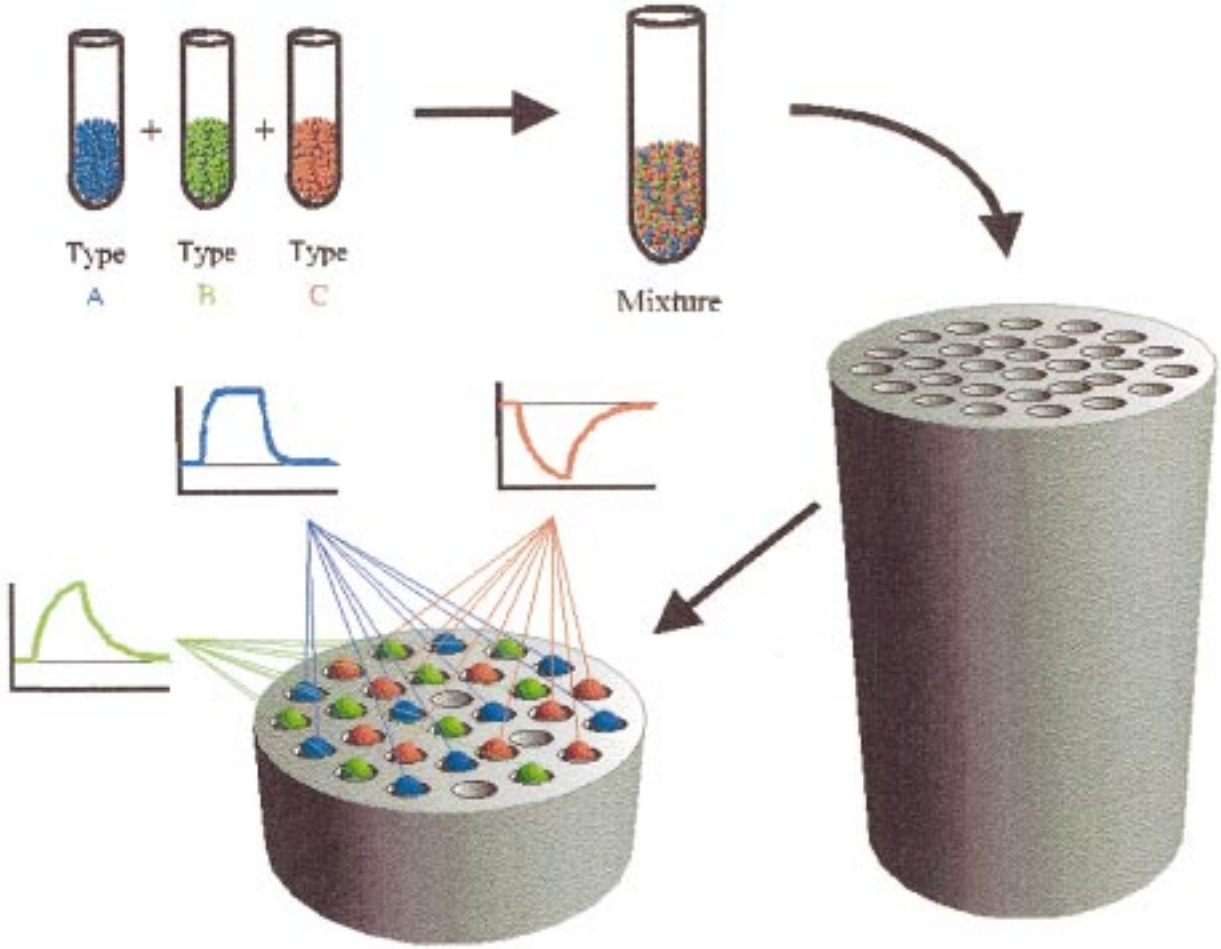

Figure 1. Schematic depiction of the self-encoded bead array (SEBA) concept. A mixture of sensor beads is prepared by combining aliquots from three stock solutions each containing a different type of polymer/dye sensor suspended in a Nanopure water/0.01% Tween solution. A drop of the final mixture is then placed onto the distal tip of an etched imaging fiber. After they have settled in random locations throughout the well array, the beads are identified and categorized by their characteristic responses to a test vapor pulse, without the need for any additional encoding schemes. Because the analytical signal of each bead is used also to identify the bead and map its position in the array, we refer to the beads as self-encoded.

responses were calculated by dividing the average intensity change over the course of the vapor pulse (frames 11−30) by the standard deviation of the baseline (frames 1−10).

RESULTS AND DISCUSSION

In the present array design, the distinct intrinsic-response characteristics of each class of bead sensor eliminates the need for an additional encoding system. Since each bead type has its own unique response to a given vapor, the beads can easily be recognized after they have been placed into the image guide wells simply by exposing the array to a known test vapor and matching the resulting temporal-response plots to those obtained beforehand for each bead class (Figure 1). Here, it is the intrinsic chemical and physical natures of the various bead types that, in conjunction with a solvatochromic dye, give rise to different, unique responses to vapors and thus serve to differentiate one bead sensor from another. Because each bead's analytical signal is also its encoding signal, we refer to these sensor arrays as self-encoded bead arrays (SEBA).

Sensor beads are incorporated into an optical array using a technique described previously.[24] Briefly, optical image guides (500-μm diameter) comprised of ~5000 hexagonally packed, coherently drawn optical fibers (each with a 3.5-μm diameter) serve as the platform for the array. Because the composition of the cladding differs from that of the glass cores, hydrofluoric acid can be used to selectively etch the cores of the image guide, leaving 5000 microwells of 3.5-μm diameter across the face of the fiber.[28] The prefabricated sensor beads (between 3.0 and 3.4 μm) can then be deposited into the wells by placing a droplet (150 nL) of solution containing the beads onto the fiber tip to form a high-density, micron-scale array of up to 5000 individual sensors, each fully addressable through its own light channel. Beads are held securely within the wells, presumably, through electrostatic interactions, eliminating the need for sophisticated immobilization schemes. This fabrication approach is simple and inexpensive, allowing thousands of sensor beads to be assembled into an array with a diameter of less than a millimeter without the need for micromachining, photolithography, photodeposition, or other sophisticated means of microfabrication. In addition, unlike electronic devices, the individual elements need not be individually wired: one excitation light beam simultaneously addresses all sensing elements.

(28) Pantano, P.; Walt, D. R. *Chem. Mater.* **1996**, *8*, 2832.

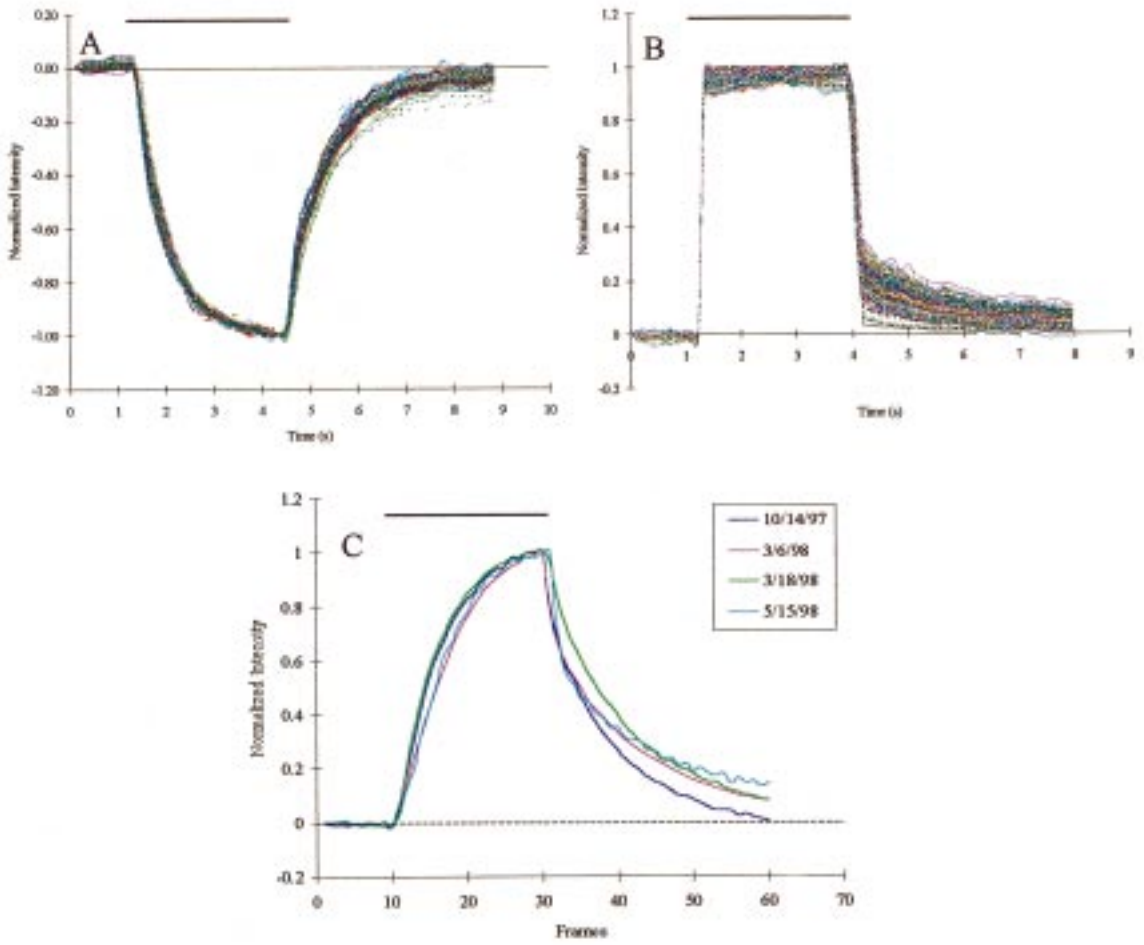

Figure 2. Normalized temporal responses of three different bead types assembled in separate image guide microwell arrays: (A) 100 Type-C beads, response to saturated methanol vapor monitored at 620 nm with 485-nm excitation light; (B) 215 Type-A beads response to saturated ethyl acetate vapor (640-nm emission, 535-nm excitation). Array to array repeatability is shown in (C) with responses from four different fiber arrays to saturated methanol vapor pulses, each prepared with bead-type B at different times over the course of seven months (dates of sensor fabrication and testing are given in the legend; for all data shown in part C, 640-nm emission and 535-nm excitation were used; each trace represents the average of 5−10 beads). Black bar denotes vapor-pulse duration.

With the growing number of bead-based applications, particularly in the areas of combinatorial synthesis, chromatography, and clinical diagnostic assays, monodisperse polymer microspheres are now commercially available with narrow, well-characterized size distributions. These microspheres are available in large quantities (~6 billion beads/mL) with a high degree of uniformity within any one bead type. The bead format thus allows for the rapid, simple preparation of a virtually unlimited number of identical sensors. Parts A and B of Figure 2 demonstrate this sensor-response reproducibility across large numbers of like beads in two separate arrays upon exposure to vapor pulses. Although we have not yet completed a thorough investigation of multibead array repeatability, data obtained from four separate arrays containing the same bead type, fabricated on different occasions over the course of several months, demonstrate a remarkable consistency in response shape (Figure 2C), suggesting that the fabrication of nearly identical, multibead-type arrays should be possible. The ability to produce sensors in a reproducible fashion is critical to the success of an artificial-nose device in order to avoid time-consuming retraining of the neural network each time a new sensor array is incorporated into the device. As with biological systems, an artificial nose would ideally continue to expand its knowledge base over time as new odors are encountered, eventually accumulating an extensive database from which to draw when making future odor classifications. All chemical sensors, both biological and artificial, have a finite lifetime. In many vertebrate species, for example, olfactory receptor cells are thought to survive for a period of 4−8 weeks (depending on the species) before being replaced by new cells.[29] Despite this constant turnover, the sense of smell appears to remain stable, and the memory of scents previously experienced is retained. In rats, for example, odor memory and learned odor discriminations can be retained for weeks to months.[30] Similarly, the continued use of an accumulated database (or trained network) in an artificial nose following sensor replacement will depend on the ability to produce large numbers of identical sensors that robustly maintain their response shape over time. With the present sensor arrays, for example, replacement will ultimately be required because of dye photobleaching over long periods of time (several weeks of

(29) Costanzo, R. M.; Graziadei, P. P. C. In *Neurobiology of Taste and Smell*; Finger, T. E., Silver, W. L., Eds.; Wiley: NY, 1987; p 205.
(30) Otto, T.; Cousens, G.; Rajewski, K. *Behav. Neurosci.* **1997**, *111*, 1257.

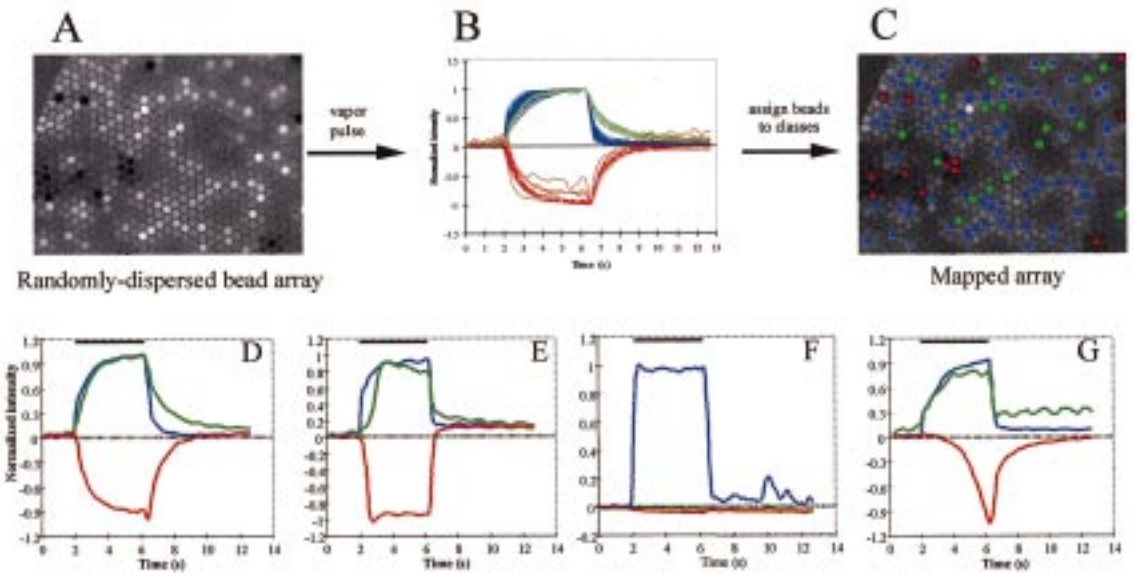

Figure 3. Data from a three-component SEBA (A). An initial pulse of methanol serves both as a vapor-sensing experiment and the array-decoding step. The three responses of the three bead types used are identified (B) to provide a map of the array (C). In this particular region of the fiber, 120 beads were identified: 88 Type A, 19 Type B, and 13 Type C. The SEBA's response to four different saturated vapors are also shown; (D) methanol, (E) dichloromethane, (F) toluene, (G) acetone. In D−G, traces represent the average response from each bead class. Prior to calculating averages, raw responses (not shown) with SNR > 3 were normalized (positive responses normalized to 1, negative responses to −1) for clearer display and to facilitate response-shape comparisons. Apparent differences in noise across different bead types are thus artifacts of the normalization process. The reduced consistency of response among the red (Type-C) beads shown in the SEBA (3B) as compared to the single-bead-type array responses shown in Figure 2A may be a result of the excitation method used for the experiment. To demonstrate the feasibility of single excitation and emission wavelength monitoring of a multibead-type array, a 510-nm (band-pass 20 nm) filter was selected in order to accommodate the somewhat separated excitation peaks of Nile Red and SensiDye (535 and 485 nm, respectively). This less than optimal excitation wavelength for the Type C-beads is probably responsible for their increased response variability, a problem which will most likely be solved with a broader excitation filter.

continuous use). The high degree of sensor reproducibility coupled with the simple and low-cost fabrication of the present sensor arrays may make the periodic replacement of the entire array a simple and cost-effective procedure that does not require network retraining.

The use of microspheres permits the fabrication of individual sensing elements and sensor arrays with dimensions that are smaller than any of those currently employed in artificial-nose devices. Miniaturization of the sensing elements not only gives rise to reductions in sensor-response times, but also appears to lead to enhanced sensor sensitivity: sensors prepared from porous silica beads, for instance, were found to have response times of ~20 ms and average signal changes of 300% when exposed to saturated ethyl acetate (with some outliers giving responses of up to 17 times). On average, a 5-s experiment is ample time for most types of bead sensors to fully respond to and recover from a pulse of vapor at any given concentration: silica bead sensors, however, can easily achieve full-cycle times of under 1.5 s. This reduction in response and recovery times may be of particular value to applications requiring higher sample throughput or real-time monitoring. In addition, such improvements in size and speed are likely to lead to new, unforeseen applications.

To demonstrate the SEBA concept, a multibead array was fabricated from a mixture of three different types of microspheres (Table 1). A fluorescence image of a region of the SEBA (~750 pixels or 15% of the total fiber face) is shown in Figure 3; fluorescence intensities across the image reveal approximately 180 wells containing beads. Beads located along the edge of the fiber and beads with intensities less than 15 counts above background were not used, yielding a final group of 120 beads. A pulse of saturated methanol vapor was delivered to the sensor array while 60 image frames were collected in rapid succession using a CCD camera. Plotting the intensity of the bead-containing wells with respect to time produced the characteristic response shapes of the three bead types present in the array. Using an imaging-software program, each bead (and its response) was assigned to one of three colors within a few seconds by manually selecting a time frame within the sequence where all three curve shapes were most clearly distinguishable from one another (in this case, frame 32, $t = 7$ s, just after the vapor pulse was turned off) and assigning threshold intensity ranges for the three bead classes. The resulting, mapped SEBA contains a multi-colored software-generated "overlay" for use in all subsequent odor-testing with the array. For example, parts D−G of Figure 3 display the average responses of the same array to various organic vapors.

Table 1. Microspheres Used in the SEBA Fabrication

bead type	ref color	dye	microsphere material	size (μm)
A	blue	Nile Red	porous silica	3.2
B	green	Nile Red	poly(methylstyrene), 12.5% divinyl benzene	3.3
C	red	SensiDye	poly(methylstyrene), 12.5% divinyl benzene	3.3

A particularly useful similarity between the natural system and the artificial device presented here is the large degree of

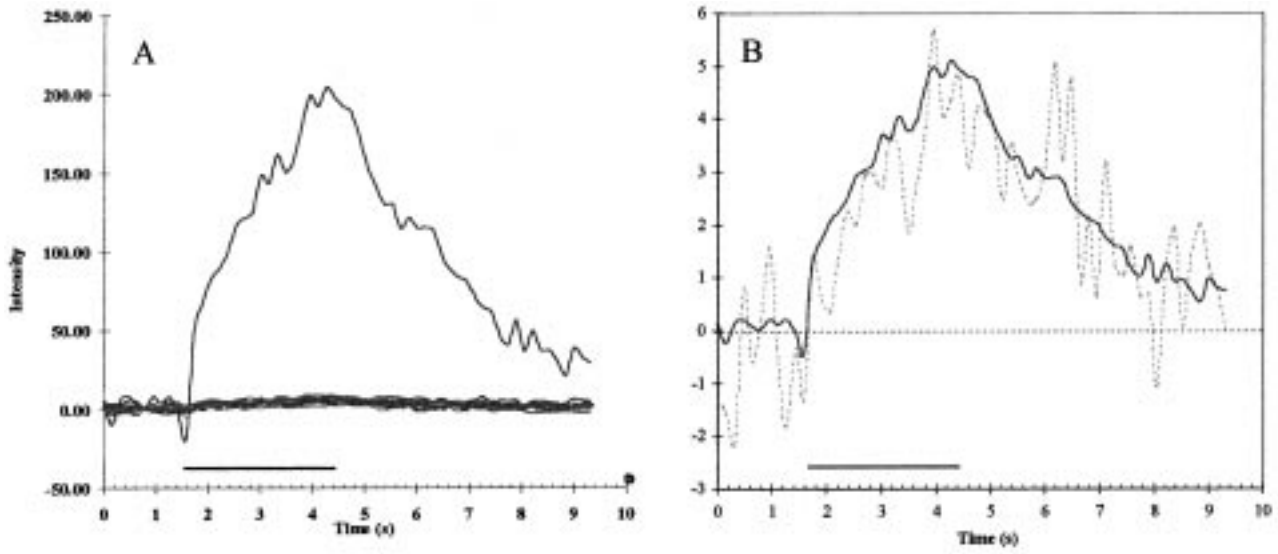

Figure 4. Signal amplification by combining bead signals from an array of polymethylstyrene (Type-B) bead sensors immobilized in an etched imaging fiber. The combined response of 39 beads in the array to methanol vapor diluted to 1% in air is shown above both in the form of (A) the sum, and (B) the average of the bead responses. The dotted trace corresponds to an arbitrarily selected single bead response and is included for comparison to the average bead response (solid trace). A 6-fold improvement in SNR was observed.

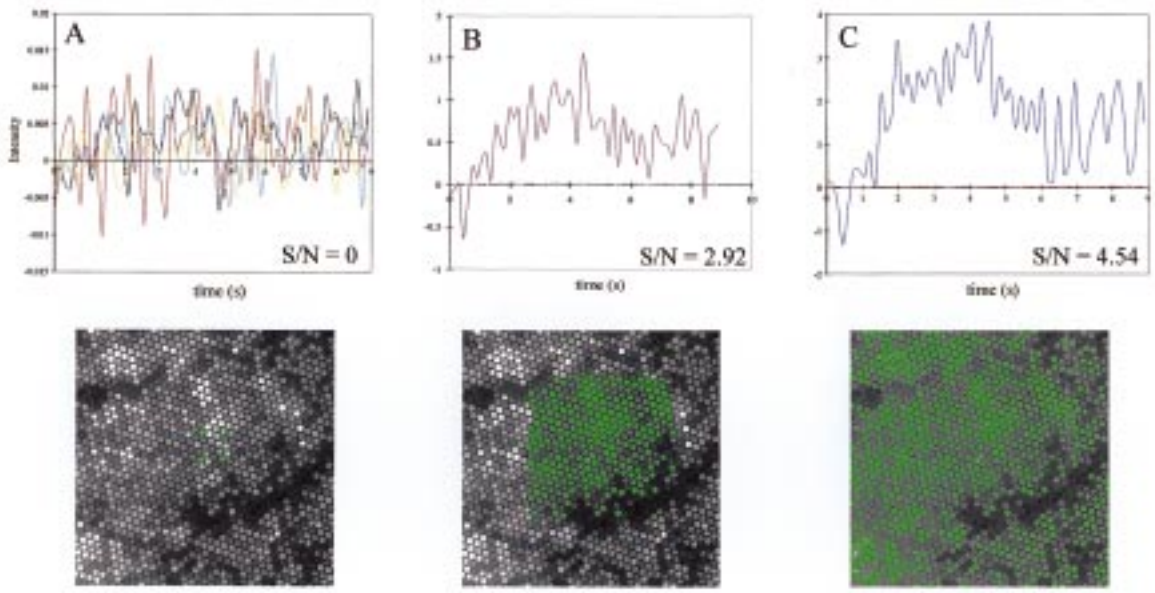

Figure 5. Top panel demonstrates signal amplification with low-level vapor concentration using an array of porous silica (Type-A) bead sensors; the response of (A) four arbitrarily selected single beads, (B) 250 summed beads, and (C) 750 summed beads to a 0.84 ppm toluene vapor pulse (0.002% in air). In this case, the combined signal from 750 beads is required to bring the signal-to-noise ratio (SNR) above 3. Each graph represents the average of three separate vapor exposures (image data of the three runs were averaged prior to SNR calculation); in addition, the average of three control runs (carrier air only) was subtracted from these responses to ensure signals were not the result of humidity or other effects. Bottom panel shows the image of the silica-bead fiber array with the various overlays used to measure the desired number of bead intensities over time. Signal-to-noise ratios of the fluorescence temporal responses were calculated by dividing the average intensity change over the course of the vapor pulse (frames 11−30) by the standard deviation of the baseline (frames 1−10).

redundancy inherent in both systems. It is thought that there are millions of receptor cells made up of approximately 1000 different receptor types in the mammalian olfactory epithelium.[31] While none of the receptors are thought to be particularly sensitive in and of themselves, it is likely that their combined signals lead to the highly sensitive and discriminative sense of smell.[32] Axons from a large number of distributed receptor cells in the epithelium have been shown to converge onto localized regions of the glomerular layer of the olfactory bulb.[33,34] The convergence of large numbers of receptor cells onto far fewer bulb elements has been proposed to result in significant amplification and noise reduction.[35] We have attempted to incorporate this naturally

(31) Buck, L.; Axel, R. *Cell* **1991**, *65*, 175.
(32) Kauer, J. S. *Trends Neurosci.* **1991**, *14*, 79.
(33) Kauer, J. S. In *Neurobiology of Taste and Smell*; Finger, T. E., Silver, W. L., Eds.; Wiley: NY, 1987; p 205.
(34) Vassar, R.; Ngai, J.; Axel, R. *Cell* **1993**, *74*, 309.
(35) Van Drongelen, W.; Holley, A.; Doving, K. B. *J. Theor. Biol.* **1978**, *71*, 39.

evolved convergence and amplification process directly into the design of the present artificial olfactory system. The large redundancy inherent in the SEBA format (i.e., the presence of hundreds or thousands of identical sensors in each array) affords the opportunity for sensitivity enhancement through signal summing in a manner similar to that believed to take place at the glomerular layer of the olfactory bulb. By combining the responses of a large number of individual microspheres, we have been able to produce large enhancements in the overall sensitivity of the array. A similar approach has been used in the field of microelectrode arrays,[36] where the advantages of microelectrodes (small size, rapid response times, small diffusion layers, and small voltage drops) are combined with an array format in order to amplify the relatively small currents generated by individual microelectrodes. In the present optically based architecture, each element is individually addressable, making it possible to combine the signals from large numbers of like elements randomly distributed throughout the array (as was done in Figure 3).

Summing the responses from n beads results in an improvement in signal-to-noise ratio (SNR) that is approximately proportional to $\sqrt{n}$ (the predicted value from basic signal-averaging theory). This feature is useful at lower vapor concentrations where signals are difficult to resolve from the baseline. In Figure 4, for example, a pure Type B bead array was exposed to a pulse of methanol vapor diluted to 1% in air (~1600 ppm), where the SNR of the individual beads was calculated to be ~2.2. Combining the signals from 39 beads resulted in an approximately 6-fold enhancement in the SNR. Figure 5 demonstrates the ability to combine hundreds of bead signals when detection of lower levels of analyte are required. Here, the silica (Type A) bead array (used in Figure 2B) was tested with a pulse of 0.84 ppm toluene vapor (a dilution of 0.002% in air). While the temporal plots from any one bead in the array exhibit no appreciable response to the vapor pulse (Figure 5A), the aggregate response of 750 beads (Figure 5C) generates an easily detectable signal (SNR, ~4.5).

This work supports the notion that mimicking naturally evolved systems such as olfaction can lead to improvements in device design and performance. The approaches presented here, including the array construct, the self-encoding system, and the signal-amplification methods employed, all are of a broad-based nature and can be extended to other analyte systems and applications such as immunoassays, high-throughput screening, and gene-probe sequencing. For these applications, as well as the development of an artificial nose, the approach is particularly attractive in that it can easily accommodate new sensors (or assays) as they are developed. For the artificial-nose field, these arrays offer improvements in size, response and recovery times, ease of preparation, sensitivity, cost, and sensor reproducibility.

ACKNOWLEDGMENT

We gratefully acknowledge Dr. Joel White for his helpful discussions and suggestions in reviewing this manuscript, Dr. Sandra Schultz for assistance with bead sensor development, and Dr. Jim La Clair for supplying the 'SensiDye'. This work was supported by the Multi-University Research Initiative (MURI) program of the US Office of Naval Research, and by the US National Institutes of Health (to JK).

Received for review December 31, 1998. Accepted March 3, 1999.

AC981457I

(36) Caudill, W. L.; Howell, J. O.; Wightman, R. M. *Anal. Chem.* **1982**, *56*, 130.